Synthesis, X-ray Structure, and Properties of 2-(1′-Pyridin-2′-one)Benzimidazole

Antonio de la Hoz,[†] Ines Almena,[†] Concepción Foces-Foces,[‡] Manuel Yáñez,[§] Otilia Mó,[§] Manuel Alcamí,[§] Nadine Jagerovic,[||] and José Elguero*[,||]

Universidad de Castilla-La Mancha, Facultad de Química, Departamento de Química Orgánica, E-13071 Ciudad Real, Spain, Departamento de Cristalografía, Instituto de Química-Física "Rocasolano", CSIC, Serrano 119, E-28006 Madrid, Spain, Departamento de Química, C-9, Universidad Autónoma de Madrid, Cantoblanco, E-28049 Madrid, Spain, and Instituto de Química Médica, CSIC, Juan de la Cierva, 3, E-28006 Madrid, Spain

Received: August 1, 2001; In Final Form: October 19, 2001

2-(1′-Pyridin-2′-one)benzimidazole was synthesized in order to determine its structure in the solid state, its NMR properties, and its behavior in absorption−emission electronic spectroscopy. To rationalize these properties, ab initio calculations have been carried out on its ground and excited states. A three-center N−H···O═C hydrogen bond connects the molecules in the crystal forming chains parallel to the *c* axis. The intramolecular hydrogen bond promotes coplanarity of both ring systems. In the ground state, only the N−H tautomer exists as a local minimum of the potential energy surface, while in the excited-state, both tautomers are found to be stable. The main consequence is that the photochemical behavior of this compound is governed by the existence of a proton transfer in its excited state.

Introduction

This work describes a first attempt to synthesize and study an "inverted ESIPT compound" (excited-state intramolecular proton transfer). The ESIPT phenomenon is present in a variety of compounds, among them heterocycles; for these last compounds, there are two possible situations, both much studied, depending on the link between the heterocycle and the *o*-phenol substituent. In compounds where both moieties are C−C linked, general structure **1** (Scheme 1; the fused benzene ring is not necessary, and many other heterocycles have been shown to present ESIPT), the proton transfer that occurs in the excited state, transforms **1a** (the hydroxy tautomer) into **1b** (the keto tautomer).[1] The second case, to which belongs Tinuvin P or TIN, corresponds to the N−C situation, which is different in the sense that the phototautomerization transforms **2a** into a zwitterion **2b**.[2] In both cases, the ground state corresponds to a phenolic structure. Here, we will describe a more radical modification where the ground state corresponds to a keto form **3a**; we have called these structures "inverted ESIPT" for obvious reasons.

Experimental Section

Synthesis. All melting points were determined on a Gallenkamp apparatus and are uncorrected.

*Compound **3a**.* In a round-bottom flask, a mixture of 2-chlorobenzimidazole (1.525 g, 10 mmol) and 2-pyridone (0.95 g, 10 mmol) was stirred at 120 °C for 24 h. The crude mixture was chromatographed on silica gel using ethyl acetate:hexane 4:1 as the eluent providing 0.838 g (40%) of **3a**. mp 202−204 °C (from dichloromethane). IR (KBr): 3263 (NH), 1666 (C═O) cm^{-1}.

SCHEME 1

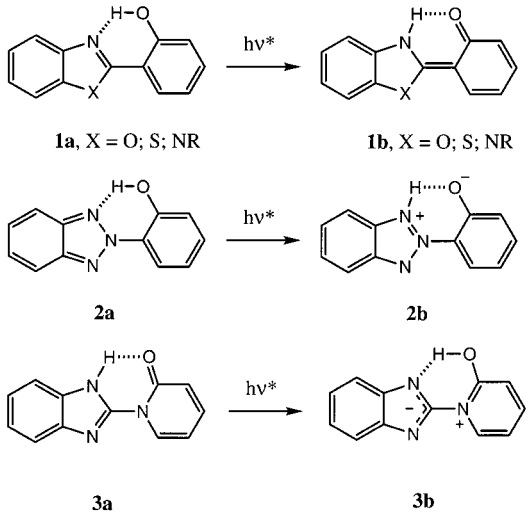

*Compound **4**.* In the same way, a mixture of 1-methyl-2-chlorobenzimidazole (0.166 g, 1 mmol) and 2-pyridone (0.095 g, 1 mmol) was stirred at 120 °C for 24 h. The crude mixture was chromatographed on silica gel, using ethyl acetate:hexane 4:1 as the eluent affording 15 mg (5%) of **4**. mp 168−9 °C. IR ($\nu_{C=O}$): 1686 cm^{-1}.

Spectrophotometry. The IR spectrum of compound **3a** was recorded in KBr between 600 and 3500 cm^{-1} using a Perkin-Elmer 883 IR Spectrophotometer. Fluorescence spectra were recorded on a Perkin-Elmer LS50B spectrometer, while UV−visible spectra were recorded on a Perkin-Elmer Lambda 16 spectrometer. Absolute ethanol (99.8%, Panreac, UV−IR spectroscopic grade) and cyclohexane (99.9%, Sigma-Aldrich, HPLC grade) were used without further purification. The excitation

* Corresponding author. Address: Instituto de Química Médica, CSIC, Juan de la Cierva, 3, E-28006 Madrid, Spain. FAX: 34-1-564.48.53. E-mail: iqmbe17@iqm.csic.es.
[†] Universidad de Castilla-La Mancha.
[‡] Instituto de Química-Física "Rocasolano", CSIC.
[§] Universidad Autónoma de Madrid.
[||] Instituto de Química Médica, CSIC.

10.1021/jp012974z CCC: $20.00
Published on Web 11/28/2001

TABLE 1: Crystal Analysis Parameters at Room Temperature

crystal data	**3a**
chemical formula	$C_{15}H_{11}NO$
crystal color	Colorless
crystal description	hexagonal Prism
crystal size (mm)	0.47 × 0.20 × 0.20
crystal system	orthorhombic
space group	P212121
no. reflections for lattice parameters	50
θrange for lattice parameters	2−45(°)
a/Å	14.7951(9)
b/Å	11.7547(6)
c/Å	5.7175(3)
packing: V(Å^3), Z	994.3(1), 4
D_c (g/cm^3), M_r, F(000)	1.411, 211.22, 440
μ (cm^{-1})	7.67
Data Dollection	
diffractometer type	Philips PW1100, graphite-oriented monochromator. CuKα radiation. Measurement time = 1 min/reflection, detector apertures = 1 × 1 (°), scan width = 1.5 (°), collection method = w/2θ scans. Two standard reflections every 90 min: no variation.
θmax(°)	65.0
no. of recorded reflections	2068
no. of independent reflections	1015
no. of observed reflections	969($I > 2\sigma(I)$ criterion)
Refinement	
refinement	least-squares on Fo, full matrix
R, ωR	0.025, 0.030
no. of parameters refined	182
weighting-scheme	empirical as to give no trends in $\langle\omega\Delta^2F\rangle>$ vs $\langle\lvert F_{obs}\rvert\rangle$ and $\langle\sin\theta/\lambda\rangle$
ratio of freedom	5.3
$(\Delta\rho)_{max}$ (e/Å^3)	0.12
⟨shift/error⟩	0.01
max. thermal value (Å^2)	U11[O^{16}] = 0.073(1)

SCHEME 2

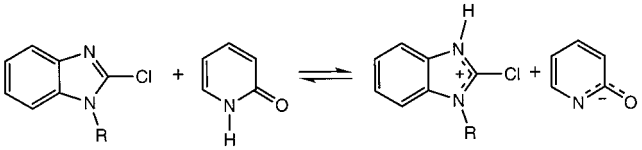

wavelengths used for the emission spectra were determined from the absorption spectra data.

NMR Spectroscopy. ^{1}H NMR and ^{13}C NMR spectra were recorded at 299.94 and 75.429 MHz, respectively, on a Varian Unity 300 spectrometer. Chemical shifts are reported in ppm (δ) using Me_4Si as standard, and coupling constants J are given in Hz. NMR simulation experiments were performed using the standard VARIAN VNMR 6.1B software.

X-Ray Crystallography. Table 1 summarizes the experimental and refinement results. The structure was solved by direct methods [3] and refined by least-squares procedures. Most of the calculations were performed using the XTAL System[4] and PARST [5] programs. The atomic scattering factors were taken from the International Tables for X-ray Crystallography, Vol. IV.[6] Cif file was deposited with the Cambridge Crystallographic Data Center (CCDC 155410).

Theoretical Calculations. Ab initio calculations have been carried out for compound **3** and for a simplified model system, **5**, where the benzimidazole group was replaced by the corresponding imidazole one. One of the objectives of the present study was to determine if the keto and enol forms are stable, i.e., if they are minima of the potential energy surface (PES). For this reason, several methods have been used to ensure the stability of our results.

For the ground state, preliminary results were obtained by fully optimizing the geometries at the HF level for compound **5**. To include correlation effects in the calculations, these geometries were refined using both perturbation theory (MP2) and density functional theory (DFT) with the B3LYP functional.[7,8] At this last level, two further calculations were performed: (a) a fully optimization of compound **3** instead of the model compound **5** to ensure the reliability of our model and (b) the inclusion of solvent effects by means of the SCPM model. Frequency calculations were performed at the B3LYP level.

TABLE 2: ^{1}H Chemical Shifts (δ) and ^{1}H−^{1}H Coupling Constants (Hz) of Compounds 3A and 4 (Solvent: DMSO-d_6)

compound	signal	δ	J
	3a		
benzimidazole	NH	12.32 (broad)	
	H-4	7.73	7.4, 1.5, 0.8
	H-5	7.33	7.6, 7.4, 2.5
	H-6	7.32	7.6, 7.2, 1.5
	H-7	7.52	7.2, 2.5, 0.8
pyridone	H-3′	6.76	9.3, 1.4, 0.8
	H-4′	7.49	9.3, 6.6, 2.2
	H-5′	6.49	7.4, 6.6, 1.4
	H-6′	8.88	7.4, 2.2, 0.8
	4		
benzimidazole	N−CH_3	3.71	
	H-4	7.79	7.1, 0.5, 0.5
	H-5	7.38	7.6, 7.1, 1.0
	H-6	7.33	7.6. 6.3, 0.5
	H-7	7.40	6.3, 1.0, 0.5
pyridone	H-3′	6.59	9.5, 1.1, 0.9
	H-4′	7.49	9.5, 6.6, 2.1
	H-5′	6.34	6.6, 6.6, 1.1
	H-6′	7.55	6.6, 2.1, 0.9

TABLE 3: ^{13}C Chemical Shifts (δ) and ^{1}H−^{13}C Coupling Constants (Hz) of Compounds 3A and 4 (Solvent: DMSO-d_6)

compound	signal	δ	^1J	^mJ	^nJ
		3a			
benzimidazole	C-2	146.57 (singlet)			
	C-3a	139.76 (multiplet)			
	C-4	118.91	169.2	7.5	
	C-5	123.27	161.8	7.5	
	C-6	122.98	160.1	7.5	
	C-7	111.51	161.6	7.6	
	C-7a	132.10 (multiplet)			
pyridone	C-2′	162.70 (multiplet)			
	C-3′	122.38	164.0	7.3	
	C-4′	132.82	187.3	6.8	
	C-5′	107.88	171.0	8.8	2.6
	C-6′	140.54	163.2	9.3	
		4			
benzimidazole	N−CH_3	30.70	141.0		
	C-2	146.57 (singlet)			
	C-3a	140.80 (multiplet)			
	C-4	120.22	162.2	5.6	2.5
	C-5	123.70	160.7	7.8	
	C-6	122.79	160.2	6.5	2.0
	C-7	109.87	171.7	9.1	3.0
	C-7a	135.33 (multiplet)			
pyridone	C-2′	161.70	−	10.6	5.0, 2.3
	C-3′	121.73	168.2	7.1	1.5
	C-4′	137.32	177.3	7.0	6.1
	C-5′	106.63	162.2	7.6	
	C-6′	141.23	162.1	9.0	

TABLE 4: Selected Geometrical Parameters (Å, deg)[a]

	exp.	CSD		exp.	CSD
N^1-C^2	1.353(2)	1.358(12)	$N^{10}-C^{11}$	1.403(2)	1.387(13)
N^1-C^9	1.379(2)	1.378(8)	$N^{10}-C^{15}$	1.387(2)	1.370(7)
C^2-N^3	1.308(2)	1.318(13)	$C^{11}-O^{16}$	1.237(2)	1.243(12)
N^3-C^4	1.391(2)	1.392(10)	$C^{11}-C^{12}$	1.433(3)	1.432(10)
C^4-C^9	1.403(2)	1.398(9)	$C^{12}-C^{13}$	1.348(3)	1.346(8)
$N^{10}-C^2$	1.418(2)	−	$C^{13}-C^{14}$	1.409(3)	1.400(11)
			$C^{14}-C^{15}$	1.344(3)	1.347(8)
$C^9-N^1-C^2$	106.1(1)	107.2(9)	$N^{10}-C^{11}-C^{12}$	115.1(2)	114.8(11)
$N^1-C^2-N^3$	114.7(2)	113.1(11)	$C^{11}-C^{12}-C^{13}$	122.5(2)	122.0(6)
$C^2-N^3-C^4$	103.9(1)	104.6(8)	$C^{12}-C^{13}-C^{14}$	120.0(2)	120.4(4)
$N^3-C^4-C^9$	110.0(2)	109.9(10)	$C^{13}-C^{14}-C^{15}$	119.5(2)	118.9(5)
$C^4-C^9-N^1$	105.3(2)	105.2(8)	$C^{14}-C^{15}-N^{10}$	121.1(2)	121.1(10)
$C^{15}-N^{10}-C^{11}$	121.8(2)	122.7(14)			
$N^1-C^2-N^{10}-C^{11}$	−3.7(3)				
$C^2-N^{10}-C^{11}-O^{16}$	2.1(3)				

hydrogen interactions	D−H	H···A	D···A	D−H···A	motif
$N^1-H^1...O^{16}$	0.93(2)	2.04(2)	2.608(2)	118(2)	S^6
$N^1-H^1...O^{16}(1/2-x,1-y,-1/2+z)$	0.93(2)	2.16(2)	2.904(2)	136(2)	C^6
$C^{14}-H^{14}...N^3(1/2-x,-y,1/2+z)$	0.97(3)	2.60(3)	3.400(2)	133(2)	C^6
$C^{13}-H^{13}...C(A)(-1/2+x,1/2-y,1-z)$	1.00(2)	2.66(2)	3.541(2)	148(2)	−

[a] C(A) represents the centroid of the C(4), C(5), ... C(9) ring. Data retrieved from the CSD are followed by the standard deviation of the sample. (CSD refcodes for the 2-benzimidazole derivatives: BZDMAZ, BZIMBF10, BZQUXL, CICVUF, CIKZUR, COTXUE, DETZEH, DIQLEU, JEYKUT, JUPKAG, LEBCUQ, LIKCEN, LIYTIW, NURQAS, REFXUV, THBDBAZ10, TOHHED, VEFVOR, WISDEH. And for 2-pyridone derivatives: BARMPN, GIQCAK, HOMDAO, JEWJUG, NCPPYO10, RFURPD, ROKPOW, RUVZAJ, SONYAV, SONJEZ, SONYOJ, SONZAW, WATZAS, ZENQUE[18].)

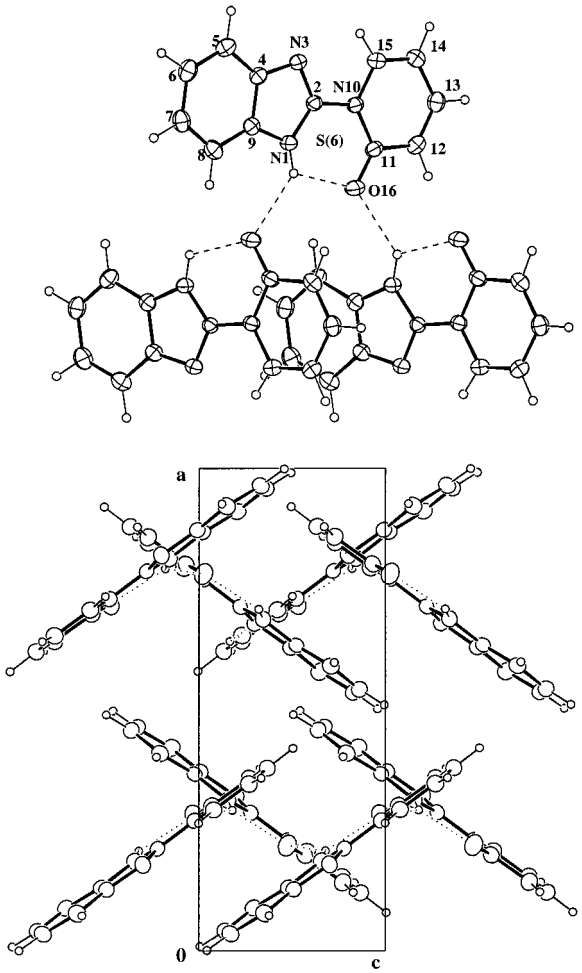

Figure 1. (a) Part of the crystal packing of **3a** showing the formation of the C(6) chain. The displacement ellipsoids are drawn at 30% probability. (b) Crystal packing of **3a** along the *b* axis.

For the excited state, geometries have been optimized at the CASSCF level.[9] Dynamical correlation effects have been included at the CASPT2 level[10] without reoptimizing the geometries. The active space in both the CASSCF and the CASPT2 calculations was selected by distributing 10 electrons among 9π orbitals. We have checked, by testing different active spaces including π orbitals, that the CASSCF and CASPT2 results for the vertical excitations are stable with such a selection of the active space. Inclusion of σ orbitals in the active space did not lead to an improvement of the results. In all cases, the 6-31G* basis set was used.

Gaussian 98 has been employed[11] for all the computations except for the CASSCF for which the MOLPRO 2000 suite of programs was used.[12]

Results and Discussion

Synthesis. Compound **3a** and its *N*-methyl derivative **4** were prepared as indicated in the experimental part; these kind of molecules where a pyridone and a benzimidazole are N−C linked were unknown, although Alcalde et al. had reported several related 2-1−pyridiniumbenzimidazoles. [13]

Synthesis of derivatives **3a** and **4** were performed by reaction of 2-chlorobenzimidazole or 2-chloro-1-methylbenzimidazole with 2-pyridone in the absence of base and solvent-free conditions. The absence of solvent enhances the nucleophilicity of 2-pyridone, while in the absence of base, the benzimidazole facilitates the reaction by activation of both the 2-pyridone and the benzimidazole (Scheme 2). A proton transfer from the pyridone to the benzimidazole results in an enhanced nucleophile (the pyridonate anion) and a good nucleofuge (the chlorine atom of the benzimidazolium cation).

This simple procedure avoids the use of reaction sequences involving protection and deprotection of the benzimidazoles and activation of 2-pyridone in basic conditions.

NMR Spectroscopy. For the NMR part, we have used the systematic numbering reported above. The ^{1}H and ^{13}C NMR results, related through 2D experiments, are presented in Tables 2 and 3.

The assignment of the ^{1}H NMR spectra was performed considering the multiplicity and coupling constants of the pyridone and benzimidazole rings. In cases where overlapping

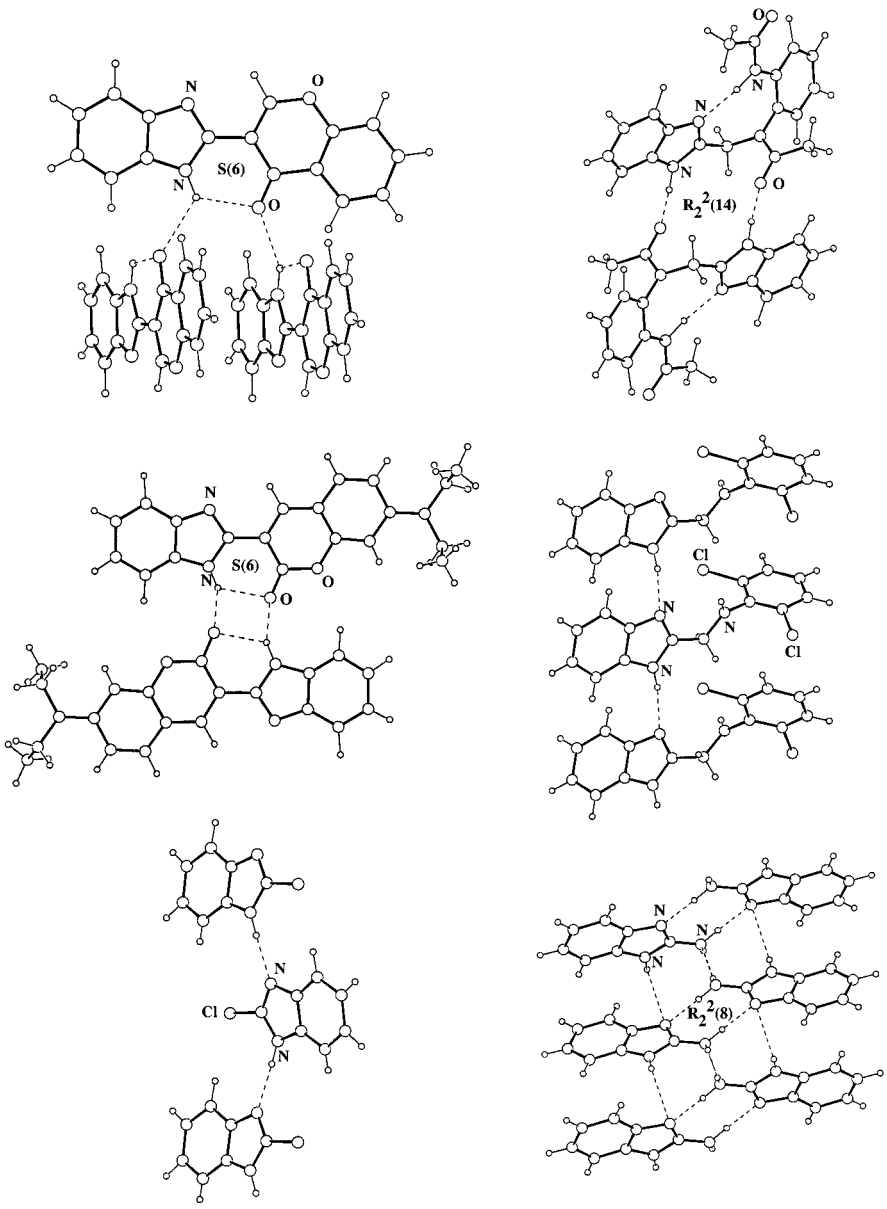

Figure 2. Partial packing diagrams illustrating the hydrogen-bonding motifs in the 2-substituted benzimidazoles compounds retrieved from the CSD. Only one N−H donor: (a) C(6) chain in DETZEH, (b) dimers in VEFVOR, and (c) C(4) chain in WISDEH. Two NH donor groups: (d) $R_2^2(14)$ dimers in COTXUE and (e) C(4) in NURQAS. More than two donor groups: (f) sheet perpendicular to the *ca* plane in DIQLEU.

of signals made the correct assignment difficult, it was performed with the help of a computer simulation. The assignment of the ^{13}C NMR spectra was carried out considering the carbon-proton correlation for all the protonated carbons of compounds **3a** and **4** as well as the long-range C−H coupling constants and long-range correlations for nonprotonated carbons. For instance, in compound **4**, C-2 was assigned by a long-range correlation with the *N*-methyl group. The assignments of Table 3 are consistent with literature data on benzimidazoles and pyridines.[13d,14−16]

The most remarkable result, both in ^1H and ^{13}C NMR, is the absence of prototropic tautomerism in **3a**. This fact, together with the observation of a very deshielded NH (12.32 ppm) and H-6′ (8.88 ppm, to be compared with 7.55 ppm for **4**), points out to a planar hydrogen-bonded structure (see X-ray discussion and theoretical calculations). This conformation situates H-6′ in the proximity of the lone pair of N-3. On the other hand, **4** should have a twisted conformation. Slow prototropic rates in the NMR time scale have been observed for other NH-benzimidazoles.[16,17]

X-Ray Crystallography. Intramolecular bond distances and angles in **3a** are in good agreement with the average values for benzimidazole derivatives with only substituents at C2 and 2-pyridone *N*-substituted derivatives (Figure 1 and Table 4) retrieved from the CSD (Cambridge Structural Database, October 2000 release).[18] The molecule as a whole adopts an almost planar conformation, the torsion angle around the central bond is −3.7(2)°, giving rise to conformational chirality.

The hydrogen-bond network has been analyzed by means of Etter's graph-set theory[19] as implemented in the RPluto program (June 2000 version).[20,21] According to the results of the basic first-level graph-set analysis involving the N−H···O and C−H···N interactions (Table 4), the crystal packing involves chains of molecules (Figure 1) joined by C−H···π interactions. Furthermore, the N−H···O intramolecular hydrogen bond, S^6 motif, stabilizes the conformation of the molecule as it happens in the analogous derivatives DETZEH [3-2−benzimidazolyl-4*H*-(1)benzopyran-4-one] and VEFVOR [3-^{2}−benzimidazolyl-7-(diethylamino)coumarin] (Figure 2a,b). However, while the secondary structure, in chains, of **3a** and DETZEH is similar,

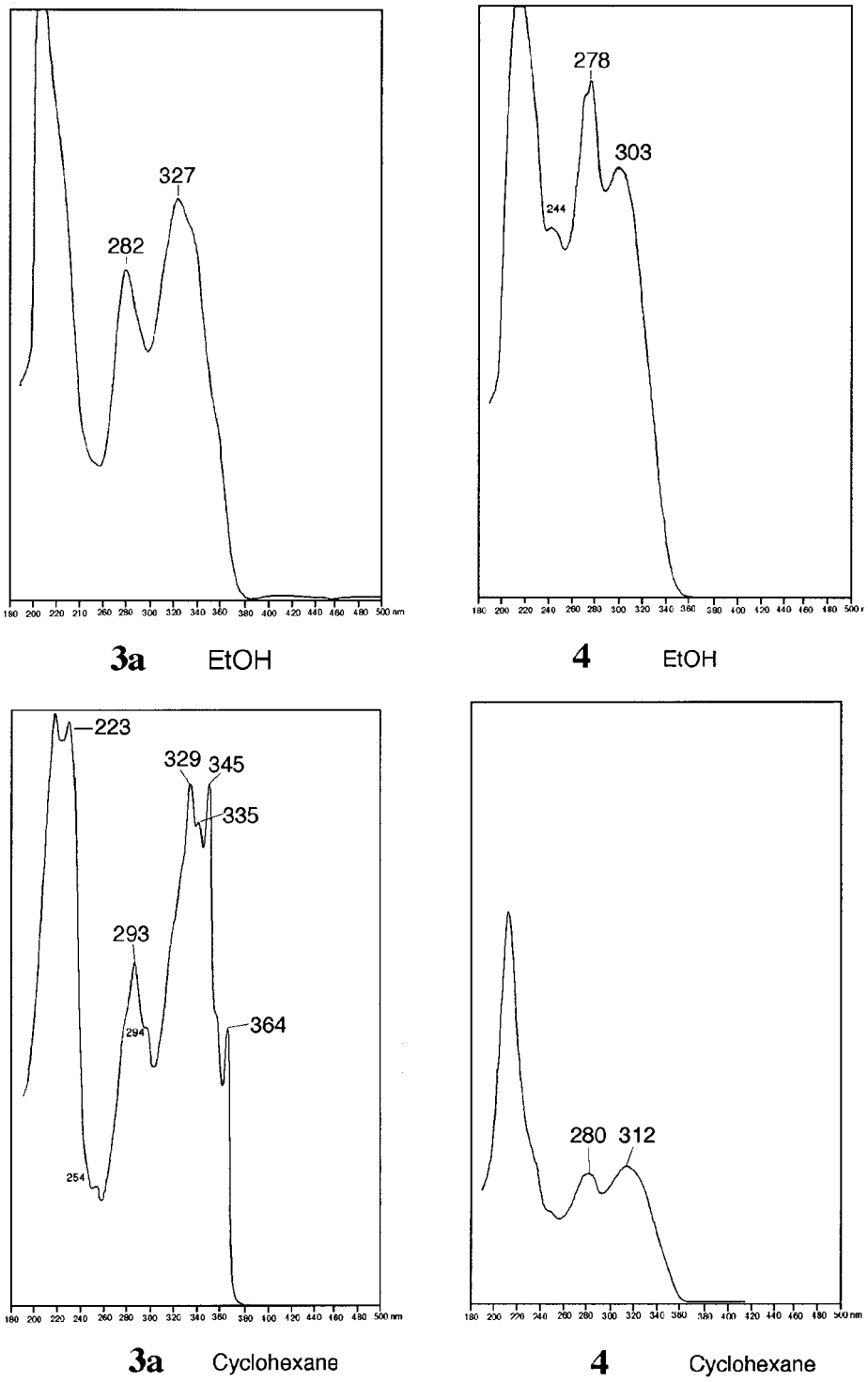

Figure 3. Absorption spectra of compounds **3a** and **4** in EtOH and cyclohexane.

the C^6 motif generated by 2-fold screw axis differs from that of VEFVOR where a ring pattern, R_2^{212} motif generated by a center of symmetry, is observed. The intra- and intermolecular hydrogen bonds in **3a** are stronger than those in DETZEH and VEFVOR with N···O distances in excess of 2.70 and 3.00 Å, respectively. In **3a**, the second-level graph-set is C_2^{210} > b > c or C_2^{212} > b < c, where b and c represent the intermolecular N−H···O and C−H···N contacts, respectively.

The graph-set analysis has also been used to describe the hydrogen bond patterns of the retrieved 2-substituted benzimidazoles in order to find out the secondary structure and whether there is a preference for a motif. Four compounds were excluded since they are salts, hydrates, or clathrates. Eight compounds, with the NH of the benzimidazole as the only donor group in the molecule, form dimers [CIKZUR, VEFVOR (Figure 2b)] and chains [C:[4] BZDMAZ, JUPKAG, THBDAZ10, WISDEH (Figure 2c); C:[6] DETZEH (Figure 2a), REFXUV].

Of the remaining compounds, those with two donor groups in the asymmetric unit form dimers [BZQUXL, COTXUE (Figure 2d)] and chains [LIYTIW, NURQAS (Figure 2e), TOHHED], while those with more than two donor groups in the asymmetric unit generate, up to a second-level, chains of dimers [DIQLEU (Figure 2f) and LIKCEN]. In these two last compounds, the remaining hydrogen bond interactions are

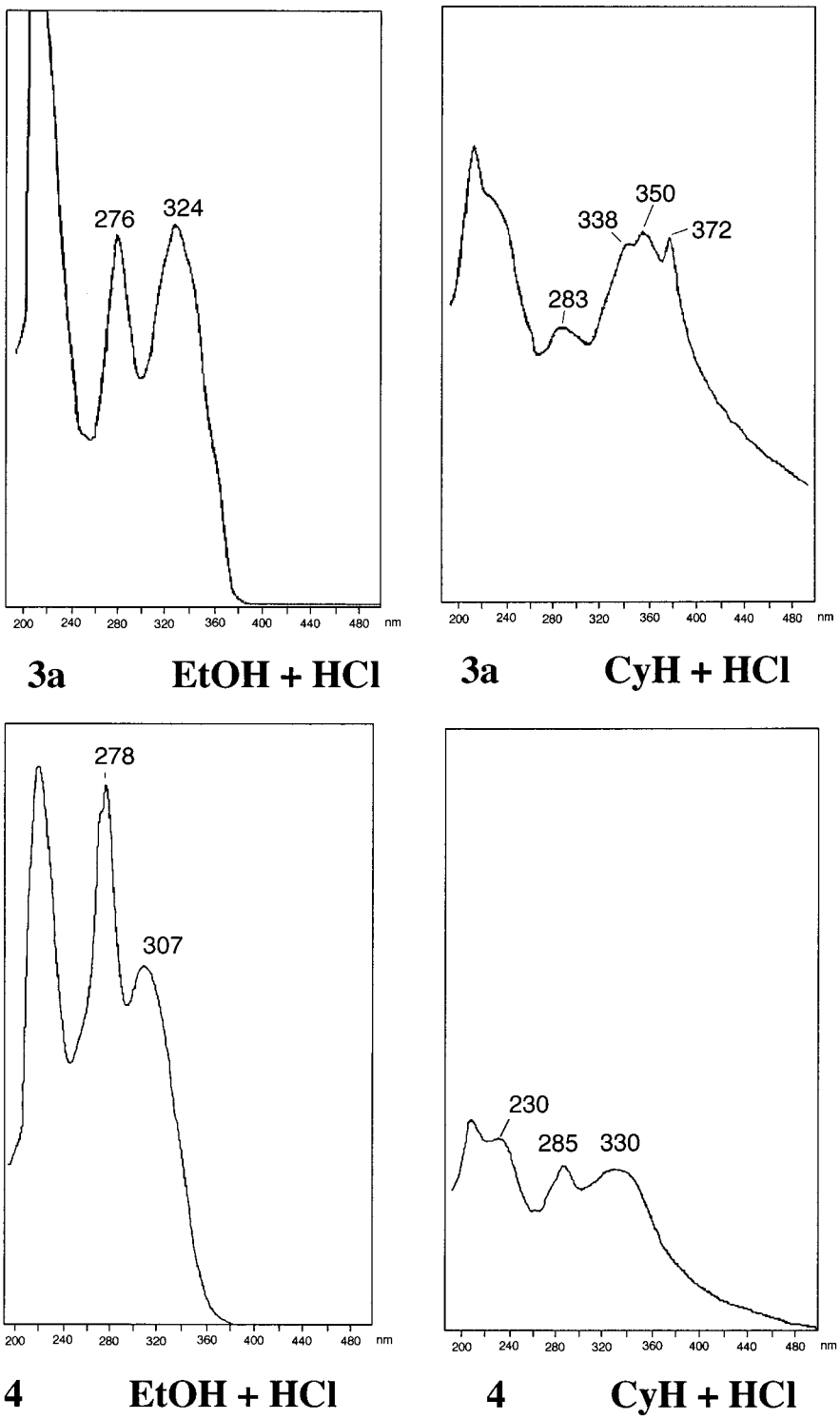

Figure 4. Absorption spectra of compounds **3a** and **4** in EtOH and cyclohexane containing a equivalent of hydrochloric acid.

responsible for connecting these chains into a sheet assembly as shown in Figure 2f. It is remarkable that in NURQAS [*N*-(1*H*-benzo(*d*)imidazol-2-ylmethyl)-*N*-2,6−dichlorophenylamine (Figure 2e)], the NH of the amide (in the substituent) plays no part in the supramolecular structure and forms a C^4 motif as in benzimidazole itself (BZDMAZ) or as in 2-chlorobenzimidazole [WISDEH (Figure 2c)].

In summary, the presence of carbonyl or hydroxyl groups at ortho position of the ring substituents (as in the title compound **3a**) always allows the formation of intramolecular hydrogen bond, S^6 motif. The chain pattern seems to be the most populated with both nitrogen atoms of the benzimidazole moiety involved in the formation of the C^4 motif, while the −N═ atoms compete with other acceptor groups present in the molecule to form the C^6 motif. Both motifs exists simultaneously when several donor and acceptor groups are present in the molecular structure.

UV Studies

The absorption and emission spectra are reported in Figures 3−6. It is clear from these spectra that the IMHB present in **3a** is destroyed by ethanol, hydrochloric acid, and, obviously, *N*-methylation (compound **4**). The fluorescence spectra results are summarized in Figure 7.

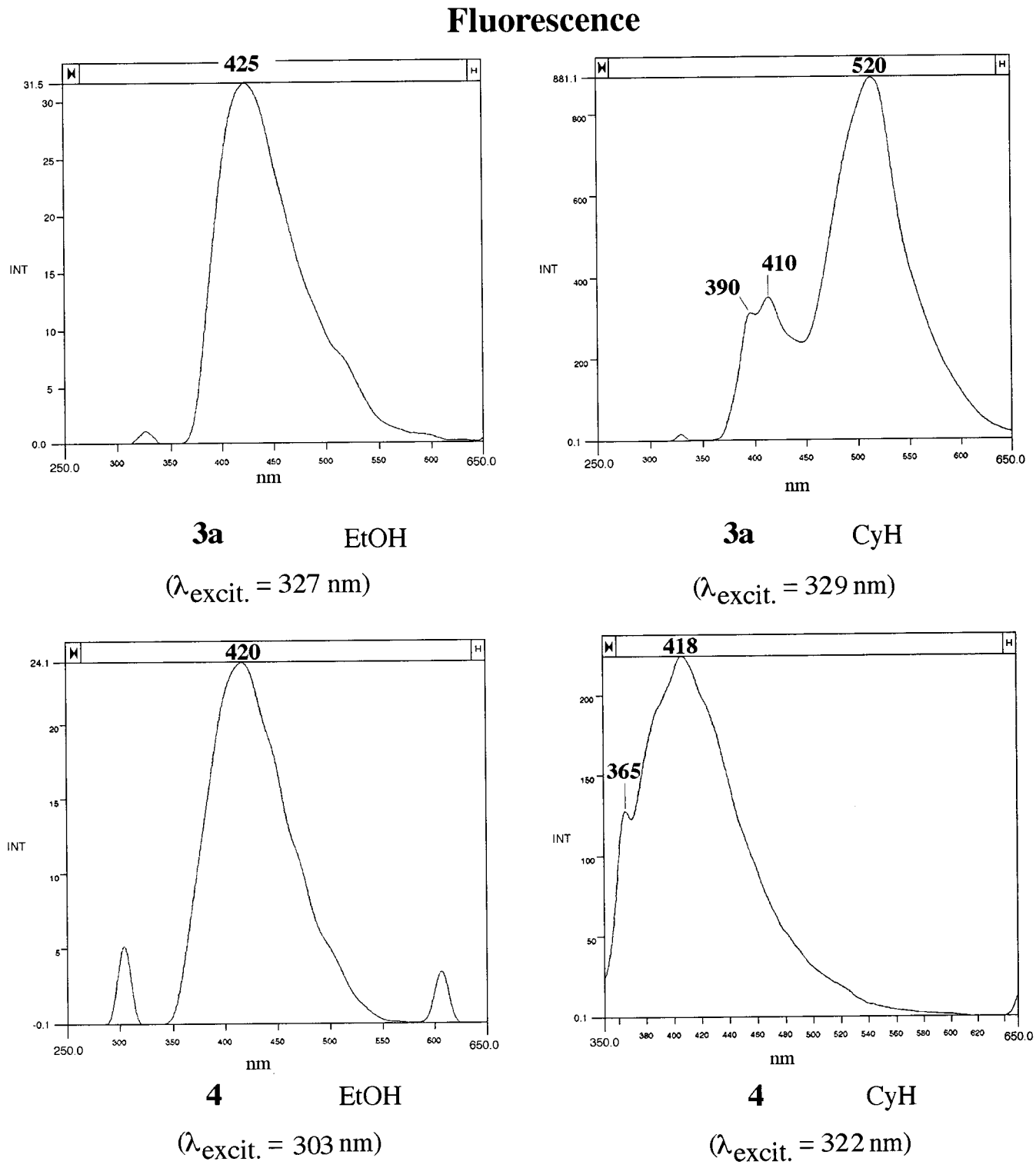

Figure 5. Emission spectra of compounds **3a** and **4** in EtOH and cyclohexane.

The emission band at 520 nm (shift of 190 nm, corresponding to a moderate Stokes shift of about 19.000 cm^{-1}) disappears in all other spectra.

Theoretical Calculations

HF/6-31G* calculations for the ground state of **5** predicts that both tautomers (**5a** and **5b**, Scheme 3) are local minima of the potential energy surface (PES), **5a** being 21 kcal mol^{-1} more stable than **5b** (Scheme 3 and Table 5). However, when these geometries were refined at the MP2/6-31G* level, the **5b** tautomer collapses with no activation barrier to the **5a** one. The conclusion reached when the MP2 method is used does not change when the calculation is carried out using the B3LYP/6-31G* approach.

To better visualize this effect and to check that not even a shallow minimum exists for structure **5b**, we have scanned the PES by fixing the NH distance and reoptimizing the rest of the geometrical parameters (Table 8). The results, presented in Figure 8, confirm that no minima corresponding to **5b** exists at the MP2 level. It can also be observed that MP2//HF calculations

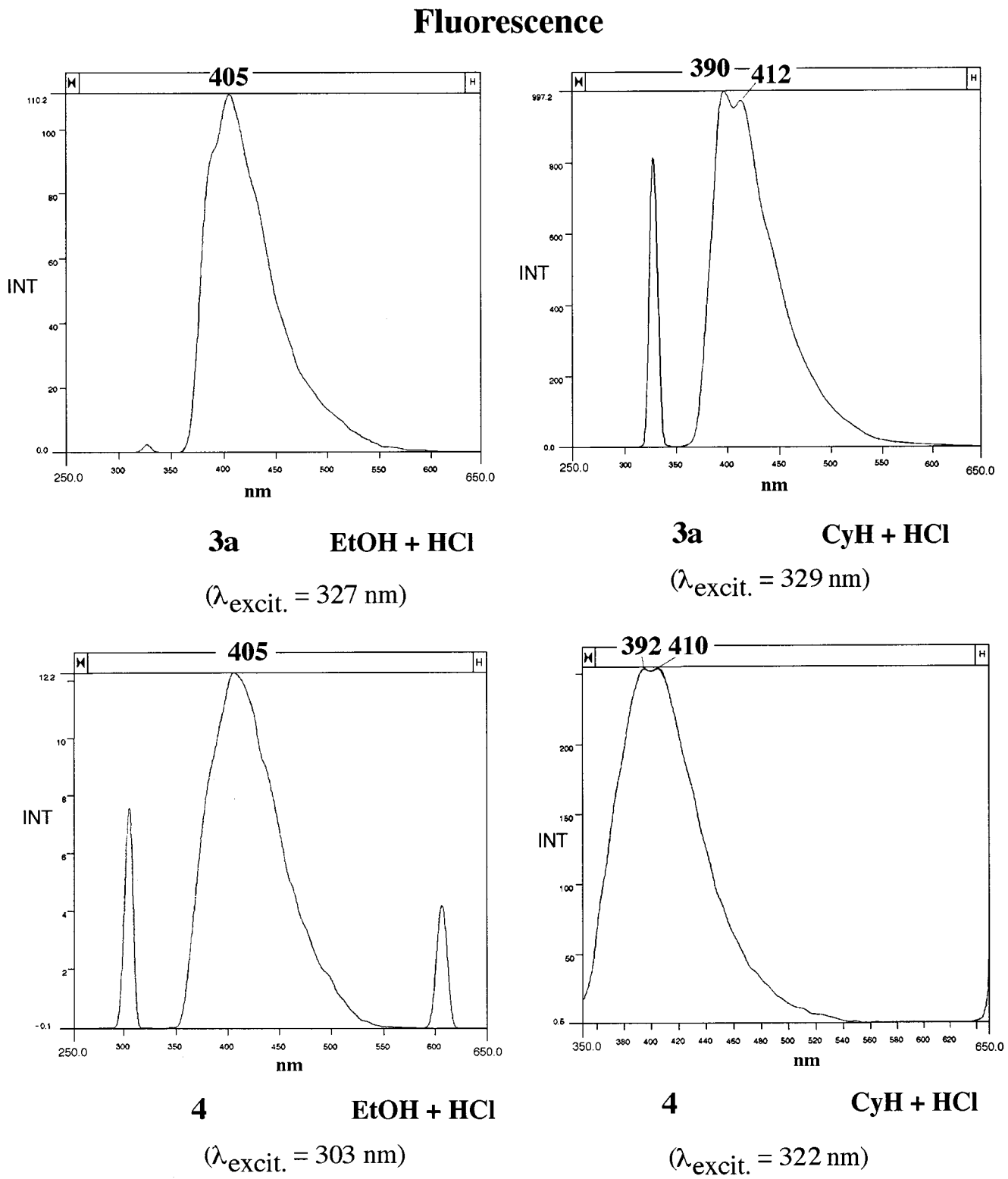

Figure 6. Emission spectra of compounds **3a** and **4** in EtOH and cyclohexane, containing an equivalent of hydrochloric acid.

give very similar values to MP2//MP2 ones, showing that even though correlation effects are important with respect to the energies, HF geometries can be considered as fairly reliable in this respect.

It is also important to note that the situation does not change when similar calculations are carried out on compound **3**. In other words, when the geometry of **3b** is optimized at the B3LYP/6-31G* level, it collapses also to the **3a** minimum. This is in agreement with ^{1}H and ^{13}C NMR spectra which, as mentioned before, show the absence of prototropic tautomerism in **3a**. The calculated geometry of **3a** (Table 5) compares very well with the experimental one. The mean deviations in the distances is 0.05 Å and in the angles 0.5°. It is important to notice that the greater difference is obtained for the $N^{1}-H^{1}\cdots O^{16}$ angle. Comparison between the geometries of compounds **5a** and **3a** shows very small differences in the bonds on the five-membered ring and nearly no difference in the bonds of the six-membered ring. More importantly, the changes in the description of the $N-H\cdots O$ bond are negligible. These results confirm that model compound **5a** is an excellent approach to describe **3a**.

TABLE 5: Experimental and Calculated Geometries for Tautomers 3a and 5a[a]

	exp.	CSD	B3LYP **3a**	B3LYP (aqueous sol.) **3a**	B3LYP **5a**	B3LYP (aqueous sol.) **5a**
N(1)−C(2)	1.353(2)	1.358(12)	1.366	1.365	1.358	1.357
N(1)−C(9)	1.379(2)	1.378(8)	1.384	1.383	1.378	1.377
C(2)−N(3)	1.308(2)	1.318(13)	1.312	1.314	1.317	1.320
N(3)−C(4)	1.391(2)	1.392(10)	1.387	1.388	1.376	1.379
C(4)−C(9)	1.403(2)	1.398(9)	1.418	1.417	1.374	1.373
N(10)−C(2)	1.418(2)		1.417	1.416	1.418	1.419
N(10)−C(11)	1.403(2)	1.387(13)	1.429	1.426	1.426	1.422
N(10)−C(15)	1.387(2)	1.370(7)	1.383	1.385	1.380	1.382
C(11)−O(16)	1.237(2)	1.243(12)	1.237	1.241	1.239	1.244
C(11)−C(12)	1.433(3)	1.432(10)	1.444	1.441	1.443	1.440
C(12)−C(13)	1.348(3)	1.346(8)	1.364	1.365	1.365	1.367
C(13)−C(14)	1.409(3)	1.400(11)	1.424	1.423	1.422	1.421
C(14)−C(15)	1.344(3)	1.347(8)	1.359	1.359	1.361	1.361
C(9)−N(1)-C(2)	106.1(1)	107.2(9)	106.9	106.4	106.5	106.8
N(1)−C(2)-N(3)	114.7(2)	113.1(11)	114.6	114.4	112.8	112.6
C(2)−N(3)-C(4)	103.9(1)	104.6(8)	104.1	104.2	104.5	104.5
N(3)−C(4)-C(9)	110.0(2)	109.9(10)	110.3	110.2	110.7	110.7
C(4)−C(9)-N(1)	105.3(2)	105.2(8)	104.8	104.8	105.4	105.4
C(15)−N(10)-C(11)	121.8(2)	122.7(14)	122.3	122.1	122.4	122.2
N(10)−C(11)-C(12)	115.1(2)	114.8(11)	114.5	114.7	114.5	114.8
C(11)−C(12)-C(13)	122.5(2)	122.0(6)	122.5	122.5	122.4	122.4
C(12)−C(13)-C(14)	120.0(2)	120.4(4)	120.3	120.2	120.3	120.1
C(13)−C(14)-C(15)	119.5(2)	118.9(5)	118.9	119.0	118.9	118.9
C(14)−C(15)-C(16)	121.1(2)	121.1(10)	121.5	121.6	121.5	121.6
N(1)−C(2)-N(10)−C(11)	−3.7(2)		0.0	0.0	0.0	0.0
C(2)−N(10)-C(11)−O(16)	2.1(3)		0.0	0.0	0.0	0.0
N(1)−H(1)	0.93(2)		1.016	1.016	1.017	1.016
H(1)−O(16)	2.04(2)		1.891	1.902	1.891	1.913
N(1)−O(16)	2.608(2)		2.596	2.597	2.593	2.598
N(1)−H(1)-O(16)	118(2)		123.7	122.8	123.3	122.0

[a] Bond lengths are in Å, and bond angles are in deg.

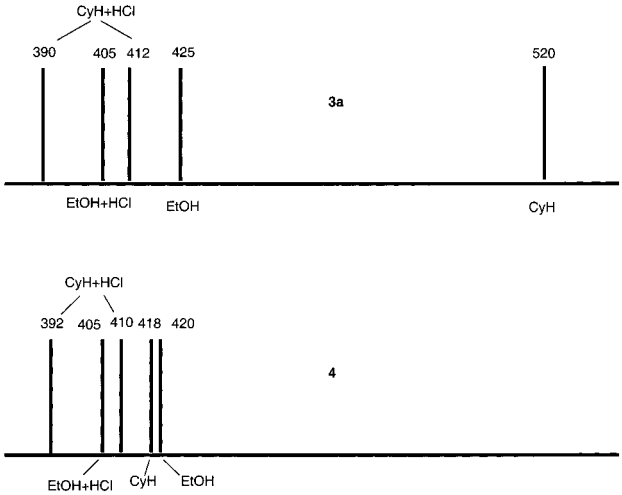

Figure 7. Schematic representation of the fluorescence spectra.

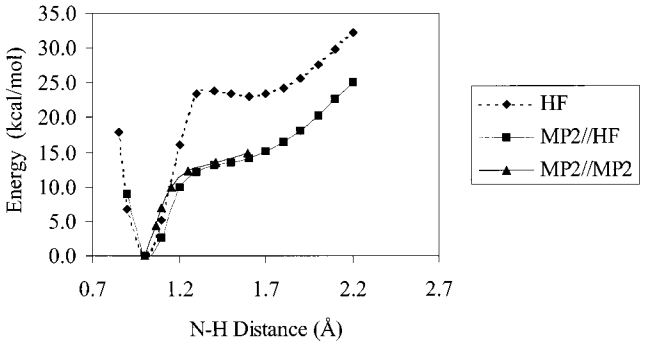

Figure 8. Potential energy curve corresponding to the hydrogen transfer process in the ground state of compound **5**. At the HF level of theory, two tautomers, namely, **5a** and **5b**, are predicted to exist. When dynamical correlation effects are included at the MP2 level, only the **5a** tautomer is found to be a local minimum.

SCHEME 3

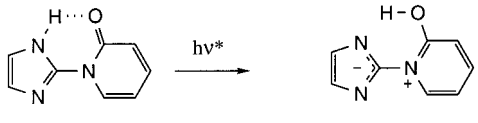

On the other hand, the good overall agreement between theoretical and experimental geometrical parameters demonstrates that the intermolecular packing effects present in the crystal induce small geometric changes.

We have also explored the possible influence of solvation effects on the relative stabilities of both tautomers. For this purpose, we have used the SCRF approach, using as dielectric constant that of water. Since the stabilities of these tautomers seem to be very sensitive to electron correlation effects, these effects were explicitly included through the use of the B3LYP method. The results obtained confirm that only tautomers **3a** and **5a** are stable in aqueous solution and (See Table 5) that its predicted geometry in the ground state does not change significantly when solvent effects are considered, the differences being on the order of 0.001 Å with respect to the unsolvated molecule.

The harmonic vibrational frequencies of **3a** obtained at the B3LYP/6-31G* level of theory have been summarized in Table 6. Although the IR spectrum of **3a** was recorded in KBr, there is a good fitting between calculated and experimental values, provided that the former have been scaled by the factor 0.9614 proposed by Scott and Radom.[22] It is worth noting that several vibrational modes in the region between 300 and 500 cm^{-1} (in bold in Table 6) lead to a significant decrease of the distance

TABLE 6: Experimental Frequencies of Compound 3 Compared with Theoretical[a,b] Ones Evaluated at B3LYP/6-31G* Level

assignment	theoretical	experimental	assignment	theoretical	experimental
a″ plane twisting	52		a′ sym. stret. C5−C6 + C7−C8	996	
a″ plane wagging	60		a′ sym. stret. C13−C14	999	1000
a″ plane twisting	129		a′ asym. stret. N1−C2 + C11−C12	1073	1079
a′plane Bending	*136*			1098	
a″ plane twisting	220			1107	1111
a″ plane bending	249			1121	
a′ **bending C11−N10−C15**	**284**			1137	1142
a′ **bending C2−N10−C11**	**317**			1159	1168
a″ plane wagging	321			1193	
a″ C− H bend. out of plane	411			1215	1232
446	1255			1255	
a′ **bending C8−C9−N1 + N10−C11−O16**	**469**			1268	1280
a″ C−H bend. out of plane	506			1296	1302
a′ ring deformation	531			1353	1359
a″ C−H bend. out of plane	563			1366	
a′ ring deformation	572		a′ C−H bending	1423	1427
	579			1434	
	611	623		1451	1442
	634			1479	
a″ C−H bend. out of plane	640			1504	1499
	692	683		1539	1542
	711			1574	1577
	731			1603	1593
	746	743		1619	1617
	748	763		1686	1666
a′ ring breathing	779	779		1977	
a″ C−H bend. out of plane	827	792		3064	
	830			3075	
a′ ring breathing	841	844		3075	
a′ ring deformation	878	858		3086	
a″ C−H bend. out of plane	894	899	a′C−H stretch.	3093	3093
a′ ring deformation	925			3111	
a″ C−H bend. out of plane	935			3113	
	935			3138	3263
	966	953		3407	

[a] Scaled by a factor of 0.9614. [b] Frequencies in bold correspond to those favoring the hydrogen transfer.

between the donor −NH group and the acceptor O, hence favoring the proton-transfer process.

Our calculations for the excited state have been restricted, for obvious reasons, to the model compound. However, in view of the results discussed above for the ground state, we may be confident on the reliability of the conclusions reached by using this simplified system. The most important finding is that while in the ground state only the **5a** tautomer is stable, in the first excited-state, both forms **5a** and **5b** are predicted to be minima of the PES at both CASSCF and CASPT2 levels (see Figure 9), structure **5b** being the global minimum. The corresponding optimized geometries are available from the authors upon request. It is important to note, however, that although the CASSCF and the CASPT2 potential energy curves are roughly parallel, dynamical correlation effects are not negligible. Indeed, while at the CASSCF method the global minimum **5b** is estimated to be 4.1 kcal mol^{-1} more stable than **5a**, at the CASPT2 level this difference is reduced to 2.3 kcal mol^{-1}. The most dramatic effects are observed as far as the isomerization barrier is concerned. At the CASSCF level, this barrier is 19.3 kcal mol^{-1} and only 5 kcal mol^{-1} at the CASPT2 level.

To evaluate the transition energies, we need to re-evaluate the potential energy curve of the ground state at the same level of theory used to describe the excited state. The corresponding CASSCF and CASPT2 curves are also shown in Figure 9. In agreement with the MP2 results discussed above, only tautomer **5a** is stable at both levels of theory.

From the CASPT2 curves of Figure 9, the vertical excitation energy is estimated to be 4.08 eV (equivalent to 303 nm), while the vertical emission energy would be 2.67 eV (equivalent to 464 nm). These values are in fairly good agreement with the experimental ones. Since both values almost equally overestimate the experimental ones, the shifting of 190 nm is quite well reproduced by our theoretical estimations (161 nm).

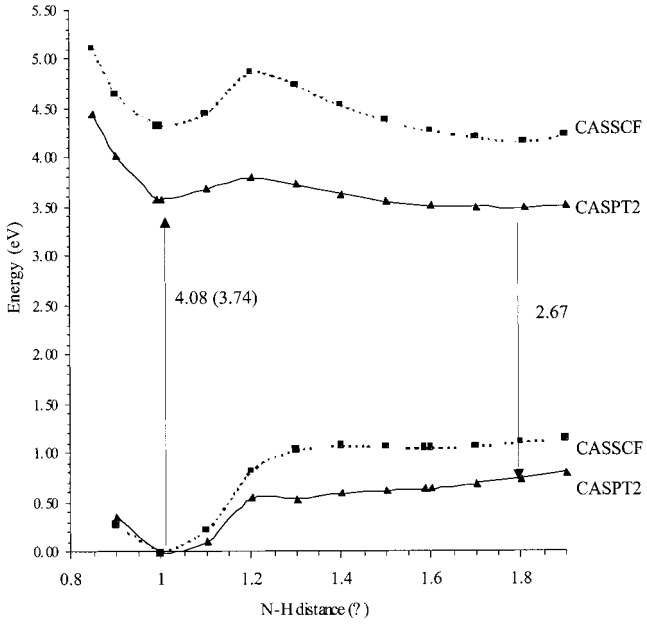

Figure 9. Potential energy curves associated with the hydrogen transfer process for compound **5**, both in the ground and in the excited states. The vertical excitation and emission energies were calculated at the CASPT2 level. The value within parentheses corresponds to the adiabatic excitation energy.

This allows us to conclude that the significant red shifting observed in the experimental UV spectrum is due to two factors. On one hand, tautomer **5b** is slightly more stable than tautomer **5a**, and the interconversion barrier between both species is rather low, and on the other hand, the ground state destabilizes significantly upon hydrogen transfer. As clearly shown in Figure 9, this last effect is the most important one in order to explain the observed shifting.

Conclusions

2-(1′-Pyridin-2′-one)benzimidazole is the first example of a compound of inverted-ESIPT structure. Both NMR and X-ray crystallography show that this compound has the necessary planar structure. In the solid state, the HB network has been analyzed by means of Bernstein's graph-set theory [S1,1(6) motif]. The compound presents a moderate Stokes shift of 190 nm (ca. 19 000 cm^{-1}) in cyclohexane. The calculations carried out at the CASPT2 level for both the ground and the excited state permit to conclude that the photochemical behavior of this compound is governed by the existence of a proton transfer in its excited state. In fact, this theoretical survey indicates that in the ground state only the N−H tautomer exists as a local minimum of the potential energy surface, while in the excited state, both tautomers are found to be stable. Furthermore, the shifting of the emission band with respect to the absorption one is essentially due to the destabilization of the system when the hydrogen transfer takes place in the ground state and, to a much lesser degree, to its stabilization in the excited state.

Acknowledgment. Dr. Roberto Sastre (CSIC) provided us access to the fluorimeter. Financial support was provided by the Spanish DGICYT (PB 97-0429, BQU-2000-0245, BQU-2000-0252, and BQU2000-0868). A generous allocation of computational time at the CCC of the Universidad Autónoma de Madrid is also acknowledged.

References and Notes

(1) [a] Catalán, J.; Fabero, F.; Claramunt, R. M.; Santa María, M. D.; Foces-Foces, C.; Cano, F. H.; Martínez-Ripoll, M.; Elguero, J.; Sastre, R. *J. Am. Chem. Soc*. **1992**, *114*, 5039. [b] Catalán, J.; del Valle, J. C.; Claramunt, R. M.; Santa María, M. D.; Bobosik, V.; Mocelo, R.; Elguero, J. *J. Org. Chem*. **1995**, *60*, 3427. [c] Douhal, A.; Amat-Guerri, F.; Acuña, A. U. *Angew. Chem., Int. Ed. Engl*. **1997**, *36*, 1514. [d] Braeuer, M.; Mosquera, M.; Pérez-Lustres, J. L.; Rodríguez-Prieto, F. *J. Phys. Chem. A* **1998**, *102*, 10736. [e] Purkayastha, P.; Chattopadhyay, N. *Phys. Chem. Chem. Phys*. **2000**, *2*, 203.

(2) [a] Catalán, J.; Fabero, F.; Guijarro, M. S.; Claramunt, R. M.; Santa María, M. D.; Foces-Foces, C.; Cano, F. H.; Elguero, J.; Sastre, R. *J. Am. Chem. Soc*. **1990**, *112*, 747. [b] Catalán, J.; Pérez, P.; Fabero, F.; Wilshire, J. F. K.; Claramunt, R. M.; Elguero, J. *J. Am. Chem. Soc*. **1992**, *114*, 964. [c] Pfeiffer, M.; Lau, A.; Lenz, K.; Elsaesser, T. *Chem. Phys. Lett*. **1997**, *268*, 258. [d] Douhal, A. *Science* **1997**, *276*, 221. [e] Catalán, J.; De Paz, J. L. G.; Torres, M. R.; Tornero, J. D. *J. Chem. Soc., Faraday Trans*. **1997**, *93*, 1691.

(3) Altomare, A.; Burla, M. C.; Camalli, M.; Cascarano, G.; Giacovazzo, C.; Guagliardi, A.; Polidori, G. SIR92, *J. Appl. Crystallogr*. **1994**, 435.

(4) Hall, S. R.; Flack, H. D. *Stewart. J. M. Xtal3.4*; University of Western Australia, Lamb: Perth, 1995.

(5) Nardelli, M. *Comput. Chem*. **1983**, 95.

(6) *International Tables for X-ray Crystallography*; Kynoch Press: Birmingham, England, 1974; Vol. IV.

(7) Becke, A. D. *Phys. Rev. A* **1988**, *38*, 3098.

(8) Lee, C.; Yang, W.; Parr, R. G. *Phys. Rev. B* **1988**, *37*, 785−789

(9) Roos, B. O. The Complete Active Space Self-Consistent Field Method and Its Applications in Electronic Structure Calculations. In *Ab Initio Methods in Quantum Chemistry*; Lawley, K. P., Ed.; John Wiley & Sons Ltd.: New York, 1987; Vol. II, pp 399−445.

(10) Andersson, K.; Roos, B. O. Multiconfigurational Second-Order Perturbation Theory. In *Modern Electronic Structure Theory. Part I*; Yarkony, D. R., Ed.; World Scientific: Singapore, 1995.

(11) Frisch, M. J.; Trucks, G. W.; Schlegel, H. B.; Scuseria, G. E.; Robb, M. A.; Cheeseman, J. R.; Zakrzewski, V. G.; J. A. Montgomery, J.; Stratmann, R. E.; Burant, J. C.; Dapprich, S.; Millam, J. M.; Daniels, A. D.; Kudin, K. N.; Strain, M. C.; Farkas, O.; Tomasi, J.; Barone, V.; Cossi, M.; Cammi, R.; Mennucci, B.; Pomelli, C.; Adamo, C.; Clifford, S.; Ochterski, J.; Petersson, G. A.; Ayala, P. Y.; Cui, Q.; Morokuma, K.; Malick, D. K.; Rabuck, A. D.; Raghavachari, K.; Foresman, J. B.; Cioslowski, J.; Ortiz, J. V.; Stefanov, B. B.; Liu, G.; Liashenko, A.; Piskorz, P.; Komaromi, I.; Gomperts, R.; Martin, R. L.; Fox, D. J.; Keith, T.; Al-Laham, M. A.; Peng, C. Y.; Nanayakkara, A.; Gonzalez, C.; Challacombe, M.; Gill, P. M. W.; Johnson, B.; Chen, W.; Wong, M. W.; Andres, J. L.; Gonzalez, C.; Head-Gordon, M.; Replogle, E. S.; Pople, J. A. *Gaussian98*, Revised A3 ed.; Gaussian, Inc.: Pittsburgh, PA, 1999.

(12) Wern, H. J.; Knowles, P. J. *MOLPRO*, 2000.1 ed.; University of Birminghan: Birmingham, U.K., 2000.

(13) [a] Alcalde, E.; Dinarés, I.; Fayet, J.-P.; Vertut, M. C.; Elguero, J. *J. Chem. Soc., Chem. Commun*. **1986**, 734. [b] Alcalde, E.; Dinarés, I.; Elguero, J.; Fayet, J.-P.; Vertut, M. C.; Miratvilles, C.; Molins, E. *J. Org. Chem*. **1987**, *52*, 5009. [c] Alcalde, E. *Adv. Heterocycl. Chem*. **1994**, *60*, 105−121. [d] Alcalde, E.; Pérez-García, L.; Dinarés, I.; Frigola, J. *Chem. Pharm. Bull. Jpn*. **1995**, *43*, 493. [e] Alcalde, E.; Gisbert, M.; Pérez-García, L.; *Chem. Pharm. Bull. Jpn*. **1996**, *44*, 29. [f] Alcalde, E.; Dinarés, I.; Pérez-García, L. *Il Farmaco* **1999**, *54*, 297.

(14) Galasso, V. *Org. Magn. Reson*. **1979**, *12*, 318.

(15) Begtrup. M.; Elguero, J.; Faure, R.; Camps, P.; Estopá, C.; Ilavsky, D.; Fruchier, A.; Marzin, C.; de Mendoza, J. *Magn. Reson. Chem*. **1988**, *26*, 134.

(16) Lee, I.-S. H.; Jeoung, E. H.; Lee, C. K. *J. Heterocycl. Chem*. **1996**, *33*, 1711.

(17) [a] Benassi, R.; Lazzeretti, P.; Schenetti, L.; Taddei, F.; Vivarelli, P. *Tetrahedron Lett.* **1971**, 3299. [b] Marzin, C.; Peek, M. E.; Elguero, J.; Figeys, H. P.; Defay, N. *Heterocycles* **1977**, *6*, 911. [c] Papadopoulos, E. P.; Hollstein, U. *Org. Magn. Reson.* **1982**, *19*, 188. [d] Alcalde, E.; Dinarés, I.; Frigola, J.; Jaime, C.; Fayet, J.-P.; Vertut, M.-C.; Miravitlles, C.; Rius, J. *J. Org. Chem*. **1991**, *56*, 4223. [e] Alcalde, E.; Dinarés, I.; Pons, J.-M.; Roca. T. *J. Org. Chem*. **1994**, *59*, 639. [f] Alcalde, E.; Gisbert, M.; Pérez-García, L. *Tetrahedron* **1995**, *52*, 13365. [g] Alcalde, E.; Alemany, M.; Gisbert, M. *Tetrahedron* **1996**, *53*, 15197. [h] Alcalde, E.; Gisbert, M.; Pérez-García, L. *Heterocycles* **1996**, *43*, 567.

(18) [a] Allen, F. H.; Davies, J. E.; Galloy, J. J.; Johnson, O.; Kennard, O.; Macrae, C. F.; Mitchell, E. M.; Smith, J. M.; Watson, D. G. *J. Chem. Info. Comput. Sci*. **1991**, *31*, 187. [b] BZDMAZ: Dik-Edixhoven, C. J.; Schenk, H.; van der Meer, H. *Cryst. Struct. Comm*un. **1973**, *2*, 23. [c] BZIMBF10: Quick, A.; Williams, D. J. *Can. J. Chem*. **1976**, *54*, 2482. [d] BZQUXL: Kanoktanaporn, S.; MacBride, J. A. H.; King, T. J. *J. Chem. Res*. **1980**, *S* 406, *M* 4901. [e] CICVUF: Caira, M. R.; Watson, W. H.; Vogtle, F.; Muller, W. *Acta Crystallogr., Sect. C* **1984**, *40*, 1047. [f] CIKZUR: Ukhin, L. Yu.; Shishkin, O. V.; Baumer, V. N.; Borbulevych, O. Ya. *Izv. Akad. Nauk SSSR, Ser. Khim.* **1999**, 566. [g] COTXUE: Armand, J.; Boulares, L.; Bellec, C.; Bois, C.; Philoche-Levisalles, M.; Pinson, J. *Can. J. Chem*. **1984**, *62*, 1028. [h] DETZEH: Rihs, G.; Sigg, I.; Haas, G.; Winkler, T. *Helv. Chim. Acta* **1985**, *68*, 1933. [i] DIQLEU: Wulff-Molder, D.; Meisel, M. Private communication, 1999. [j] JEYKUT: Gandour, R. D.; Nabulsi, N. A. R.; Fronczek, F. R. *J. Am. Chem. Soc*. **1990**, *112*, 7816. [k] JUPKAG: Mrozek, A.; Karolak-Wojciechowska, J.; Yalcin, I.; Sener, E. *Z. Kristallogr.—New Cryst. Struct*. **1999**, *214*, 181. [l] LEBCUQ: Dzvinchuk, I. B.; Vypirailenko, A. V.; Rusanov, E. B.; Chernega, A. N.; Lozinsky, M. O. *Zh. Obshch. Khim*. **1999**, *69*, 856. [m] LIKCEN: Aubry, A.; Brembilla, A.; Faivre, V.; Lochon, P. *Acta Crystallogr., Sect. C* **1995**, *51*, 115. [n] LIYTIW: Bei, F.; Jian, F.; Yang, X.; Lu, L.; Wang, X.; Shanmuga Sundara Raj, S.; Fun, H.-K. *Acta Crystallogr., Sect. C* **2000**, *56*, 718. [o] NURQAS: Eryigit, R.; Kendi, E. *J. Chem. Cryst*. **1998**, *28*, 145. [p] REFXUV: Yoshioka, N.; Irisawa, M.; Mochizuki, Y.; Kato, T.; Inoue, H.; Ohba, S. *Chem. Lett*. **1997**, 251. [q] THBDAZ10: Trus, B. L.; Marsh, R. E. *Acta Crystallogr., Sect. B* **1973**, *29*, 2298. [r] TOHHED: Elerman, Y.; Kabak, M. *Acta Crystallogr., Sect. C* **1997**, *53*, 372. [s] VEFVOR: Chinnakali, K.; Sivakumar, K.; Natarajan, S. *Acta Crystallogr., Sect. C* **1990**, *46*, 405. [t] WISDEH: Panneerselvam, K.; Soriano-García, M. *Acta Crystallogr., Sect. C* **1996**, *52*, 1799. [u] BARMPN: Hsu, I.-N.; Craven, B. M. *Acta Crystallogr., Sect. B* **1974**, *30*, 998. [v] GIQCAK: Babaev, E. V.; Bozhenko, S. V.; Maiboroda, D. A.; Rybakov, V.; Zhukov, S. G. *Bull. Soc. Chim. Belg.* **1997**, *106*, 631. [w] HOMDAO: Babaev, E. B.; Rybakov, V. B.; Zhukov, S. G.; Orlova, I. A. *Khim. Geterotsikl. Soedin*. **1999**, 542. [x] JEMJUG: Ballesteros, P.; Claramunt, R. M.; Cañada, T.; Foces-Foces, C.; Cano, F. H.; Elguero, J.; Fruchier, A. *J. Chem. Soc., Perkin Trans. 2* **1990**, 1215. [y] NCPPYO10: Wheeler, G. L.; Ammon, H. L. *Acta Crystallogr., Sect. B* **1974**, *30*, 680. [z] RFURPD: Egert, E.; Lindner, H. J.; Hillen, W.; Gassen, H. G. *Acta Crystallogr., Sect. B* **1977**, *33*, 3704. [aa] ROKPOW: Hartung, J.; Svoboda, I.; Fuess, H.; Duarte, M. T. *Acta*

Crystallogr., Sect. C **1997**, *53*, 1629. [bb] RUVZAJ: Zhukov, S. G.; Rybakov, V. B.; Babaev, E. V.; Paseshnichenko, K. A.; Schenk, H. *Acta Crystallogr., Sect. C* **1997**, *53*, 1909. [cc] SONYAV, SONYEZ, SONYOJ, SONZAW: Gericke, R.; Harting, J.; Lues, I.; Schittenhelm, C. *J. Med. Chem.* **1991**, *34*, 3074. [dd] WATZAS: Almansa, C.; Gómez, L. A.; Cavalcanti, F. L.; Rodríguez, R.; Carceller, E.; Bartrolí, J.; García-Rafanell, J.; Forn, J. *J. Med. Chem.* **1993**, *36*, 2121. [ee] ZENQUE: Banwell, M. G.; Bridges, V. S.; Hockless, D. C. R. *Acta Crystallogr., Sect. C* **1995**, *51*, 2128.

(19) [a] Etter, M. C. *Acc. Chem. Soc*. **1990**, *23*, 120. [b] Etter, M. C.; MacDonald, J. C.; Bernsteis, J. *Acta Cryst*. **1990**, *B46*, 256. [c] Bernstein, J.; Davis, R. E.; Shimoni, L.; Chang, N.-L. *Angew. Chem., Int. Ed. Engl.* **1995**, *34*, 1555.

(20) Motherwell, W. D. S.; Shields, G. P.; Allen, F. H. *Acta Crystallogr., Sect. B* **1999**, *55*, 1044.

(21) Motherwell, W. D. S.; Shields, G. P.; Allen, F. H. *Acta Crystallogr., Sect. B* **2000**, *56*, 466.

(22) Scott, A. P.; Radom, L. *J. Phys. Chem.* **1996**, *100*, 16502.